Published in final edited form as:
Hepatology. 2012 March ; 55(3): 846–855. doi:10.1002/hep.24757.

Plasma Cells and the Chronic Nonsuppurative Destructive Cholangitis of Primary Biliary Cirrhosis

Toru Takahashi[1], **Tomofumi Miura**[1], **Junichiro Nakamura**[1], **Satoshi Yamada**[1], **Tsutomu Miura**[1], **Masahiko Yanagi**[1], **Yasunobu Matsuda**[2], **Hiroyuki Usuda**[3], **Iwao Emura**[4], **Koichi Tsuneyama**[5], **Xiao-Song He**[6], and **M. Eric Gershwin**[6]

[1]Division of Gastroenterology and Hepatology, Nagaoka Red Cross Hospital, Nagaoka, Niigata, Japan

[2]Division of Human Physiological Science, Department of Medical Technology, School of Health Sciences, Faculty of Medicine, Niigata University, Niigata, Niigata, Japan

[3]Division of Medical Technology, Nagaoka Red Cross Hospital, Nagaoka, Niigata, Japan

[4]Division of Pathology, Nagaoka Red Cross Hospital, Nagaoka, Niigata, Japan

[5]Department of Diagnostic Pathology, Graduate School of Medical and Pharmaceutical Research, Toyama University, Toyama, Toyama, Japan

[6]Division of Rheumatology, Allergy and Clinical Immunology, University of California, Davis, CA, USA.

Abstract

There has been increased interest in the role of B cells in the pathogenesis of primary biliary cirrhosis. Although the vast majority of patients with primary biliary cirrhosis have antimitochondrial antibodies, there is no correlation of antimitochondrial antibody titer and/or presence with disease severity. Further, in murine models of primary biliary cirrhosis, it has been suggested that depletion of B cells may exacerbate biliary pathology. To address this issue, we have focused on detailed phenotypic characterization of mononuclear cell infiltrates surrounding the intrahepatic bile ducts of patients with PBC, PSC, AIH, CH-C and GVHD, including CD3, CD4, CD8, CD20, CD38 and immunoglobulin classes, as well as double immunohistochemical staining for CD38 and IgM. Interestingly, CD20 B lymphocytes, which are a precursor of plasma cells, were found in scattered locations or occasionally forming follicle-like aggregations but were not noted at the proximal location of chronic nonsuppurative destructive cholangitis. In contrast, there was a unique and distinct coronal arrangement of CD38 cells around the intrahepatic ducts in primary biliary cirrhosis but not controls; the majority of such cells were considered plasma cells based on their expression of intracellular immunoglobulins, including IgM and IgG, but not IgA. Patients with primary biliary cirrhosis who manifest this unique coronal arrangement were those with significantly higher titers of antimitochondrial antibodies. These data collectively suggest a role of plasma cells in the specific destruction of intrahepatic bile ducts in primary biliary cirrhosis and highlight the increasing interest in plasma cells and autoimmunity.

Correspondence to: Toru Takahashi, M.D., Director, Uonuma Hospital, Jonai 4-1-38, Ojiyashi, 947-0028, Niigata, Japan.; telephone 81-258-83-2870; fax 81-258-83-4789; torutoru@uonumahosp.jp. Toru Takahashi: torutoru@uonumahosp.jp Tomofumi Miura: tomiura@east.ncc.go.jp Junichiro Nakamura: ichirojn@nagaoka.jrc.or.jp Satoshi Yamada: yamasato@nagaoka.jrc.or.jp Tsutomu Miura: tmiura@nagaoka.jrc.or.jp Masahiko Yanagi: yanagi@nagaoka.jrc.or.jp Yasunobu Matsuda: Yasunobu@med.niigata-u.ac.jp Hiroyuki Usuda: usuda@nagaoka.jrc.or.jp Iwao Emura: emura@nagaoka.jrc.or.jp Koichi Tsuneyama: ktsune@med.u-toyama.ac.jp Xiao-Song He: xiaosong@stanford.edu M. Eric Gershwin: megershwin@ucdavis.edu.

Keywords

antimitochondrial antibodies; primary biliary cirrhosis; plasma cells; coronal arrangement

Although there has been considerable effort on defining the pathophysiology of primary biliary cirrhosis (PBC) (1), there remains an interesting void, the relative role of distinct lymphoid populations in chronic nonsuppurative destructive cholangitis (CNSDC) associated with chronic portal inflammation. Indeed the most disease-specific serologic autoantibodies in all of human immunopathology are antimitochondrial antibodies (AMA) found in greater than 95% of patients with PBC, primarily targeted at the E2 component of the pyruvate dehydrogenase complex (PDC-E2) (2). However, despite the significant value of both AMAs and elevated serum IgM in the diagnosis of PBC, there is no correlation of sera AMA or IgM with either disease severity or any other clinical features. Further, in murine models of PBC, the clinical usage of anti-CD20 antibody, aimed at depleting B cells, has not been successful and, in another murine model of PBC, depletion of B cells results in escalating liver disease, suggesting that B cells suppress the inflammatory response in mouse models (3, 4).

We have investigated the immunohistochemical distribution of liver-infiltrating B lymphocytes in liver biopsy specimens from patients with PBC and control liver diseases using monoclonal antibody (mAb) reagents specific for CD20 and CD38. We report herein a unique coronal arrangement of $CD38^+$ cells that is accompanied by CNSDC. Further, this coronal arrangement of $CD38^+$ cells is positively correlated with AMA titer and inversely correlated with serum γ-glutamyl transpeptidase (γ-GTP) levels. These $CD38^+$ cells primarily express intracellular IgM or IgG, suggesting a pathogenic role of plasma cells in PBC.

Materials and Methods

Patients

A total of 78 patients were enrolled in this study. These included 26 patients with PBC, which AMA were positive in 20 and negative in 6; 27 patients with chronic hepatitis C (CH-C), 8 patients with autoimmune hepatitis (AIH), 8 patients with PSC, and 9 patients with GVHD. The CH-C control group was assembled by age- and gender-matched subjects to the PBC group, randomly selected from a cohort of 136 candidates of interferon therapy for CH-C. The diagnosis of all cases was based on established criteria for PBC (5), AIH (6), PSC (7) and GVHD (8) respectively, or by detection of serum hepatitis C virus RNA by polymerase chain reaction for CH-C. Informed consent in writing was obtained from each patient and the study protocol was approved by the Institutional Committee for Human Research of Nagaoka Red Cross Hospital. The clinical details of patients are presented in Table 1. Liver tissue was available from all patients either from laparoscopic liver biopsies or ultrasound guided needle liver biopsies.

Liver histology and clinical data collection

Liver biopsy specimens were fixed in 10% formalin, dehydrated and embedded in paraffin. Five-μm sections were cut in a microtome and subjected to subsequent routine histological staining of silver impregnation, hematoxylin-eosin and diastase-resistant periodic acid Shiff. Histological staging based on established criteria for PBC (5), CH-C (9), AIH and PSC (10) respectively was performed by a pathologist who was blinded for all clinical data. Blood biochemical data were obtained from each patient within one week of liver biopsy. These include aspartate aminotransferase (AST), alanine aminotransferase (ALT), alkaline

phosphatase (ALP) and γ-GTP. Total bilirubin, indirect bilirubin, total protein, serum albumin, total cholesterol (TC), triglyceride, serum levels of IgG, IgA, and IgM, AMA titer and antinuclear antibody titer were included in the PBC cohort. AMA was examined by immunofluorescence and by titration with enzyme-linked immunosolvent assay (ELISA) with known positive and negative standards throughout. Antinuclear antibodies were determined by immunofluorescence on Hep2 cells.

Immunohistochemistry

Immunohistochemistry of liver biopsy was performed with a Ventana HX System BenchMark/20 (Ventana Medical Systems Inc., Tucson, Arizona, USA) which utilizes avidin-biotin-peroxidase complex (ABC) coupled with formulated unmasking pretreatment for each targeted antigen. For unmasking CD antigens and pankeratins, liver sections were soaked in Tris-EDTA buffer pH 8.5 (Ventana CC1 standard solution) at 100 °C for 60 minutes. For unmasking immunoglobulin, liver sections were soaked in Protease 1 solution (pronase 0.5 units/ml) for 8 minutes. Endogenous peroxidase activity in liver tissue was blocked by soaking specimens in 3% H_2O_2 methanol solution for 10 minutes. Non-immunized mouse IgG was used as a negative control in each experiment, which did not result in any non-specific staining signal. The following mouse monoclonal antibodies were used in this study: anti-CD3 (clone PS1), anti-CD4 (clone 1F6), anti-CD8 (clone 1A5) and anti-CD38 (clone SPC32) from Novacastla Laboratories (Newcastle upon Tyne, UK); anti-CD20 (clone L26) and anti-pankeratin (clone AE1/AE3) from Dako (Glostrup, Denmark); anti-human IgG (clone A57H), anti-human IgA (clone CB1-10.4/B8) and anti-human IgM (clone R1/69) from Nichirei Corp. (Tokyo, Japan). After incubation with each of these primary antibodies at an appropriate dilution with 5% bovine serum albumin (BSA), slides were rinsed three times with phosphate buffered saline (PBS), and then incubated with biotinylated anti-mouse IgG secondary antibodies. The slides were rinsed three times and then incubated with ABC reagents for staining of CD antigens and pankeratin. For staining of immunoglobulins, we used standard peroxidase labeled streptavidin-biotin. Diaminobenzidine hydrochloride was used as a substrate for colorimetric reaction.

Portal tracts and bile ducts were counted per specimen with pankeratin staining using AE1/AE3 monoclonal antibodies that specifically stain bile ducts and bile ductules. Portal tracts with more than half of its circumference and proper bile ducts were only counted and ductular reactions were excluded from this count. The bile ducts with coronal arrangement of $CD38^+$ cells were enumerated per specimen and the frequency of this finding amongst the total counted bile ducts was thence calculated.

For CD38 and IgM double immunohistochemical staining, mouse monoclonal anti-CD38 (SPC32) and rabbit polyclonal anti-IgM (Pierce Biotechnology, Rockford, USA) were used as previously described (11). After de-paraffinization, sections were soaked in target retrieval buffered saline (Tris, pH 6.1, Dako Cytomation, Carpinteria, CA, USA) in a plastic pressure cooker containing no metals and irradiated in a microwave oven for 10 minutes, soaked in 3% H_2O_2 methanol solution for 5 minutes, and then soaked in 5% BSA for 1 minute. A cocktail of anti-CD38 and anti-IgM antibodies were diluted to a pre-determined optimal concentration in PBS containing 5% BSA. The diluted antibodies were applied to tissue sections in a moist chamber and irradiated intermittently for 10 minutes (250W, 4 seconds-on, 3 seconds-off). After 3 washes with Tris-buffered saline containing 1% Tween 20 (TBS-T) for 1 minute, a cocktail containing peroxidase-conjugated (Envision System, Dako Cytomation) or alkaline phosphatase-conjugated secondary antibodies (Simple Stain System, Nichirei, Japan) were applied to specimens in the moist chamber. Irradiation was then performed intermittently for 10 minutes, as described above. After washing 5 times with TBS-T, the sections were immersed in Fast blue (alkaline phosphatase substrate kit, SK-5300, Vector, Burlingame, CA, USA) and 3-amino-9-ethylcarbazole (AEC) (peroxidase

substrate kit, Nichirei) and counterstained with Hematoxylin (Dako Cytomation). After substrate reaction, $CD38^+$ cells were blue and IgM^+ cells were red-brown.

Statistics

The Mann-Whitney U test was used for comparing the blood biochemical and serological data among PBC, CH-C AIH, PSC and GVHD groups and between PBC patients with or without coronal arrangement of $CD38^+$ cells; *p* values under 0.05 were considered statistically significant. The Chi-square test was used for comparing the occurrence of lymph follicle-like infiltration and the infiltration of $CD4^+$ or $CD8^+$ cells into cholangioepithelium amongst the PBC, CH-C, AIH, PSC and GVHD groups.

Results

Clinicopathological profiles of PBC, CH-C, AIH, PSC and GVHD subjects are summarized in Table 1.

Therapies for 26 PBC patients varied according to the nature and severity of the disease. Ursodeoxycholic acid (UDCA) was administered in 25 cases (96.2%) where the daily dose of UDCA was 300mg in one, 600mg in 22, and 900mg in 2 patients. Bezafibrate was also administered in 4 patients at a daily dose of 400mg, all of whom simultaneously took UDCA. Prednisolone was given in 2 cases in whom a hepatic form of PBC was noted on liver pathology. None of the 26 PBC patients progressed into the icteric stage that would need liver transplantation during the observation period through September 2011.

Histologic evaluations of liver biopsy sections revealed typical CNSDC and epithelioid cell granulomas in patients with PBC but not any of the control liver diseases (Table 2). The incidence of CNSDC in PBC was 50% (13/26) and that of granulomas was 23.1% (6/26). In contrast, lymph follicle-like infiltration was most frequently found in CH-C livers (12/27, 44.4%) but also found at lower frequencies in PBC (6/26, 23.1%) and AIH (2/8, 25%). These findings were not found in PSC or GVHD.

The distribution of lymphoid elements is summarized in Table 2. In PBC, $CD20^+$ B lymphocytes, the precursor of plasma cells, were found either scattered or aggregated within the lymphoplasmocytic infiltration (Figure 1A). Such $CD20^+$ B cells occasionally formed follicle-like aggregations but importantly they were not observed in the proximity of CNSDC (Figure 2B). In contrast, an intense coronal arrangement (CA) of $CD38^+$ cells was found around intrahepatic bile ducts in each and every specimen with CNSDC (Figures 1B and 2C) but never found in the portal tracts with ductopenia. $CD3^+$ pan-T cells were randomly scattered around CNSDC (Figure 2A), an area where $CD20^+$ B lymphocytes had not been observed (Figure 2B) while the most typical coronal arrangement of $CD38^+$ cells were found (Figure 2C). This coronal arrangement of $CD38^+$ cells was continuously present along with CNSDC since serial liver sections also demonstrated the same coronal arrangement along CNSDC (Figure 2D). $CD4^+$ and $CD8^+$ T lymphocyte infiltration was observed either in proximity of, or within the degenerated cholangioepithelium, suggesting the participation of these cells in the destructive processes of intrahepatic bile ducts (Figure 2E and 2F). This $CD4^+$ and $CD8^+$ T lymphocyte infiltration into cholangioepithelium was also observed in CH-C, AIH, PSC and GVHD cases as a consequence of lymphocytic cholangitis (Table 2).

To determine if the coronal arrangement pattern of $CD38^+$ cells is specific for PBC, we examined $CD20^+$ and $CD38^+$ cells in liver sections with other liver diseases. In CH-C, $CD20^+$ B lymphocytes were aggregated in a follicle-like fashion in the inflamed portal tracts (Figure 3A) where intrahepatic bile ducts were often centered (an arrow in Figure 3A); in

contrast, $CD38^+$ cells were found at the periphery of inflamed portal tracts but were not found around the intrahepatic bile ducts (an arrow in Figure 3B). Similarly, in AIH, $CD38^+$ cells were not observed in the proximity of intrahepatic bile ducts (BD, arrows in Figure 3C) but were abundantly infiltrated in the area of interface hepatitis (Figure 3C). In contrast to PBC livers in which $CD38^+$ cells formed coronal arrangement around an intrahepatic bile duct (BD) with CNSDC (Figure 3D), such pattern was not observed in the disease control groups including CH-C, AIH and PSC but only observed in one bile duct of one GVHD case (Table 2), although the frequency of this finding was only 0.9% (1/107) of all evaluated bile ducts in this group and thought to be incidental. In PBC livers, the coronal arrangement of $CD38^+$ cells was observed in 21.5% (7.1 - 41.0% per specimen) of all evaluated bile ducts when present (69 bile ducts among 321 counted bile ducts in the PBC group with coronal arrangement of $CD38^+$ cells). In PSC livers, $CD38^+$ cells were found surrounding, or in the onion skin-like fibrosis, a pattern that is unique in PSC (Figure 3E, F).

To determine the identity of the $CD38^+$ cells that formed a coronal arrangement specifically in the PBC livers with CNSDC (Figure 2C), we first examined the expression of immunoglobulin classes in consecutive sections of PBC livers with CNSDC by staining for immunoglobulin classes. The majority (8/13, 61.5%) of the coronal arrangements had IgM^+ cells (Figure 4C)), followed by IgG^+ cells (5/13, 38.5%) (Figure 4A). Three cases (23.1%) had both IgG^+ and IgM^+ cells in the same coronal arrangement (Figure 4) while 2 cases had only IgG^+ cells but not IgM^+ cells. IgA^+ cells were not observed in a coronal arrangement (Figure 4B). IgG^+ cells were relatively loosely scattered around CNSDC (Figure 4A), while IgM^+ cells showed dense and prominent coronal arrangement around CNSDC (Figure 4C). These results indicate that the B cells expressing antibodies participate in the formation of the coronal arrangement in CNSDC.

Next we used double immunostaining to examine the co-localization of CD38 and IgM in the same cells that comprise the coronal arrangement. The majority (up to 70%) of $CD38^+$ cells in coronal arrangement that were specifically stained by Fast blue also showed positive red-brown staining of intracellular IgM (arrows in Figure 5). These results suggest that the majority of $CD38^+$ cells were IgM plasma cells. Finally, we examined the correlation of coronal arrangement with blood biochemical and serological parameters in PBC (Table 3). Among 14 parameters, the presence of coronal arrangement was significantly associated with higher titers of AMA (p=0.0153) and lower levels of γ-GTP (p=0.0256) (Figure 6).

Discussion

The study of plasma cells in autoimmune diseases has led to the hypothesis that plasma cells with pathogenic potential are long-lived, dependent on finding a niche within a local microenvironment, i.e. such as the biliary tract. Indeed, in murine lupus BAFF, APRIL, IL-6 and adhesion molecules, all modulate the survival of plasma cells and lead to further inflammation (12-16). In organ specific autoimmune diseases such as PBC, the role of plasma cells has not attracted significant attention. Herein, we demonstrated a relatively non-specific follicle-like aggregation in inflamed portal tracts of $CD20^+$ B cells and, more importantly, a prominent coronal arrangement of $CD38^+$ plasma cells surrounding the intrahepatic bile ducts with CNSDC. CD20 is a type III membranous protein of 297 amino acids (17), which is a representative B lineage cell marker that disappears from the cell surface when B cells are differentiated into antibody-producing plasma cells. Therefore, the differential distribution of $CD20^+$ and $CD38^+$ cells in a target tissue reflects the disease-specific movement of these two cell types during B cell maturation in the course of a chronically evolving inflammatory disease such as PBC.

Our findings suggest a PBC-specific dynamic settlement in B cell lineage populations during the inflammatory processes in portal tracts, which involve migration of B lymphocytes from the portal tracts to the intrahepatic bile ducts during the maturation process from $CD20^+$ mature B cells to professional antibody-producing $CD38^+$ cells, or plasma cells. We did not, however, examine $CD38^+$ cells in cirrhotic livers of patients with PBC. Future studies should focus on a longitudinal analysis and/or detailed cross-sectional analysis of patients at different stages of disease. Also, this concept of plasma cells infiltrating environmental niches needs further exploration in other liver diseases, including expanding the data base of PSC and including patients with hepatic allograft rejection post-OLT and chronic GVHD post-HST.

The most important finding of this study is the coronal arrangement pattern of $CD38^+$ cells around the intrahepatic bile ducts with CNSDC. This pattern is specific for PBC, but not observed in other autoimmune liver diseases including AIH, PSC and GVHD, or in CH-C. CD38 is part of nicotinamide adenine dinucleotide cyclase (18). It is a type II membranous protein of 300 amino acids. CD38 expression is limited to the cell surface of T cell progenitors, lymphoid stem cells, plasmablasts and mature plasma cells. We conclude that the majority of $CD38^+$ cells observed around the intrahepatic bile ducts are mature plasma cells rather than T cell subsets based on the following observations: 1) the distribution of $CD38^+$ cells and that of IgM- and/or IgG-bearing cells were nearly identical; 2) the distribution of $CD3^+$, $CD4^+$ and $CD8^+$ T cells and that of $CD38^+$ cells were very different; 3) mature plasma cells express higher levels of CD38 than other B or T cell subsets that are $CD38^+$ (19, 20); 4) the distribution of $CD138^+$ cells, a marker more specific for mature plasma cells than CD38, was similar to that of $CD38^+$ cells (data not shown); and 5) most importantly, the double immunostaining of CD38 and IgM in PBC livers clearly indicate that approximately 70% of $CD38^+$ cells expressed IgM. However, there remains a possibility that the observed $CD38^+$ population was a mixture of diverse cell types including activated T cells, other B lineage cell populations, NK cells and basophils in addition to mature plasma cells (21). Even if this is the case, the fact that $CD38^+$ cells clearly form a coronal arrangement surrounding CNSDC strongly suggests that the coronal arrangement is related to the pathogenesis of PBC.

The role of T cell lineage populations in the pathogenesis of PBC has been extensively studied (1, 22-31). In contrast, the role of B cell lineage populations in PBC is not clear. Recently it has been shown that AMA is required in the production of inflammation cytokines by macrophages in the presence of apoptotic human intrahepatic biliary epithelial cells (32). This could explain the biliary specificity of autoimmune damage in PBC. It is possible that at different stages of PBC, B cells play different roles in the breakdown of tolerance and development of small bile duct pathogenesis. Although we cannot exclude the possibility that the formation of coronal arrangement is a consequence of, rather than a contributing factor to the destruction of small bile ducts, our data is in agreement with the findings of Lleo et al (32) which strongly suggest an active role of AMA in the inflammatory responses at the affected local bile ducts. Future studies should focus on the antigen specificity of the IgM and IgG produced in these coronal arrangement-comprising plasma cells. Although IgA transcytosis has been considered one of the contributing factors of bile duct lesions in PBC (33, 34), it is unlikely that the coronal arrangement we observed in this study includes IgA^+ plasma cells. However, we observed that IgA staining was often seen in the degenerated cholangioepithelium of CNSDC or at the apical margin of damaged bile duct cells (data not shown).

There are two steps in lymphocyte recruitment and chemotaxis in PBC: “tethering” and transendothelial migration of peripheral blood lymphocytes (PBL) from vessels to the inflamed area of liver, and recruitment and settlement of liver infiltrating lymphocytes (LIL)

around bile ducts where they participate in the destruction process of targeted bile ducts. Induced or upregulated expression of MIG and IP10 in portal tracts are thought to contribute to T cell recruitment into PBC liver (35). Once these cells have entered the portal tract, they often form lymphoplasmocytoid aggregates. Lymphoid neogenesis depends on the interaction between CCL21 (36) and MAdCAM-1 (37) expressed on high endothelial venules and on lymphatic vessels and CCR7 expressed on lymphocytes (38). The lymphoplasmocytoids are then recruited to, and retained around bile ducts by the combinational or sequential action of several chemokines (35, 39, 40). In the case of the B cells, only CXCL12 (stromal cell-derived factor 1, SDF-1) has been reported to participate in the recruitment of $CD19^+$ B cells (41-43); however CD19 is expressed in intermediate and mature B cells but not in plasma cells.

CXCL12 (SDF-1) is expressed constitutively in bile duct cells and may have a role in lymphocyte retention via its ability to augment their adhesion to fibronectin by triggering $\alpha_4\beta_7$-mediated binding of LIL (38, 44, 45). Moreover, the biliary basement membrane has immunoreactive fibronectin in 80% of PBC patients but not in other disease or normal control livers (46). We previously found that fibronectin was abundantly expressed in necrotic and newly fibrosing areas, or the area of inflammation (47), suggesting that fibronectin may contribute to the chemotaxis of $CD38^+$ cells in interface hepatitis in CH-C and AIH liver as well as in coronal arrangement in PBC livers. In addition, we have shown that the expression of alternatively spliced fibronectin containing a cell attachment specific domain (CS-1 fibronectin) was increased in fibrotic human liver (48); hence it may also contribute to the recruitment and retention of LIL through not only the $\alpha_1\beta_4$ but also the $\alpha_4\beta_7$ integrin. Taken together, these previous findings suggest that CXCL12 might be involved in the formation of coronal arrangement of $CD38^+$ cells around bile ducts. Other potential contributing factors for the formation of coronal arrangement include hepatocyte growth factor (49), LFA-1/ICAM-1 (50, 51), CXCL13 and CXCL5 (52), which should also be explored in future studies.

Although AMA is well established as a diagnostic criterion for PBC, serum AMA titer has not been correlated with any parameter of disease activity. We observe for the first time that the titer of AMA was correlated significantly with the formation of a coronal arrangement by $CD38^+$ plasma cells in the liver, which could be a bridge that links AMA and the inflammatory reactions in PBC. Although the implication of this novel correlation needs to be further studied, we propose that the plasma cells may be a source of both AMA and elevated serum IgM. UDCA is reported to decrease the level of total IgM and IgM AMA but not of IgG AMA (53). Thus, UDCA may preferably affect the $CD38^+$ plasma cells that comprise coronal arrangement. The relationship of reduced γ-GTP with the coronal arrangement is unclear since another biliary enzyme, ALP did not correlate with the coronal arrangement. Finally, the concept of an environmental niche for long-lived plasma cells and their impact on inflammation has implications not only for PBC, but from a generic perspective, in other autoimmune diseases as well; this concept has been recently reviewed (54).

Acknowledgments

We would like to give many thanks to Mr. Kyuji Iwamoto for his technical assistance in preparing histological sections and immunohistochemistry.

Funding support provided by National Institutes of Health grant DK39588.

Abbreviations

PBC	primary biliary cirrhosis
CNSDC	chronic nonsuppurative destructive cholangitis
AMA	antimitochondrial antibodies
PDC-E2	E2 component of the pyruvate dehydrogenase
mAb	monoclonal antibody
γ-GTP	γ-glutamyl transpeptidase
PSC	primary sclerosing cholangitis
GVHD	graft-versus host disease
CH-C	chronic hepatitis C
AIH	autoimmune hepatitis
RNA	ribonucleic acid
AST	aspartate aminotransferase
ALT	alanine aminotransferase
ALP	alkaline phosphatase
TC	total cholesterol
ELISA	enzyme-linked immunosolvent assay
USA	United States of America
ABC	avidin-biotin-peroxidase complex
EDTA	ethylenediaminetetraacetic acid
UK	United Kingdom
BSA	bovine serum albumin
PBS	phosphate buffered saline
CA	California
TBS-T	Tris-buffered saline containing 1% Tween 20
AEC	3-amino-9-ethylcarbazole
UDCA	ursodeoxycholic acid
BD	bile duct
BAFF	B cell-activating factor
APRIL	a proliferation inducing ligand
IL	interleukin
OLT	orthotopic liver transplantation
HST	hematopoietic stem cell transplantation
NK	natural killer
PBL	peripheral blood lymphocyte
LIL	liver infiltrating lymphocyte

MIG	monokine induced by interferon γ
IP10	interferon g-inducible protein 10
MAdCAM-1	mucosal adressin cell adhesion molecule-1
SDF-1	stromal cell-derived factor-1
CS-1	a cell attachment specific domain 1
LFA-1	lymphocyte function-associated antigen 1
ICAM-1	intercellular adhesion molecule-1

References

1. Kaplan MM, Gershwin ME. Primary biliary cirrhosis. N Engl J Med. 2005; 353:1261–1273. [PubMed: 16177252]
2. Gershwin ME, Mackay IR, Sturgess A, Coppel RL. Identification and specificity of a cDNA encoding the 70 kd mitochondrial antigen recognized in primary biliary cirrhosis. J Immunol. 1987; 138:3525–3531. [PubMed: 3571977]
3. Dhirapong A, Lleo A, Yang GX, Tsuneyama K, Dunn R, Kehry M, Packard TA, et al. B cell depletion therapy exacerbates murine primary biliary cirrhosis. Hepatology. 2011; 53:527–535. [PubMed: 21274873]
4. Moritoki Y, Zhang W, Tsuneyama K, Yoshida K, Wakabayashi K, Yang GX, Bowlus C, et al. B cells suppress the inflammatory response in a mouse model of primary biliary cirrhosis. Gastroenterology. 2009; 136:1037–1047. [PubMed: 19118554]
5. Scheuer P. Primary biliary cirrhosis. Proc R Soc Med. 1967; 60:1257–1260. [PubMed: 6066569]
6. Hennes EM, Zeniya M, Czaja AJ, Parés A, Dalekos GN, Krawitt EL, et al. Simplified criteria for the diagnosis of autoimmune hepatitis. Hepatology. 2008; 48:169–176. [PubMed: 18537184]
7. Lindor, KD.; LaRusso, NF. Primary sclerosing cholangitis.. In: Schiff, ER.; Sorrell, MF.; Maddrey, WC., editors. Schiff's Diseases of the LIver. 9thed.. Lippincott Williams & Wilkins; Philadelphia: 2003. p. 673-684.
8. Alpini G, McGill JM, LaRusso NF. The pathobiology of biliary epithelia. Hepatology. 2002; 35:1256–1268. [PubMed: 11981776]
9. Desmet VJ, Gerber M, Hoofnagle JH, Manns M, Scheuer PJ. Classification of chronic hepatitis: diagnosis, grading and staging. Hepatology. 1994; 19:1513–1520. [PubMed: 8188183]
10. Ludwig J. Surgical pathology of the syndrome of primary sclerosing cholangitis. Am J Surg Pathol. 1989; 13(Suppl 1):43–49. [PubMed: 2699167]
11. Kumada T, Tsuneyama K, Hatta H, Ishizawa S, Takano Y. Improved 1-h rapid immunostaining method using intermittent microwave irradiation: practicability based on 5 years application in Toyama Medical and Pharmaceutical University Hospital. Mod Pathol. 2004; 17:1141–1149. [PubMed: 15167936]
12. Liu Z, Zou Y, Davidson A. Plasma cells in systemic lupus erythematosus: The long and short of it all. Eur J Immunol. 2011; 41:588–591. [PubMed: 21341259]
13. Oracki SA, Walker JA, Hibbs ML, Corcoran LM, Tarlinton DM. Plasma cell development and survival. Immunol Rev. 2010; 237:140–159. [PubMed: 20727034]
14. Cassese G, Lindenau S, de Boer B, Arce S, Hauser A, Riemekasten G, Berek C, et al. Inflamed kidneys of NZB / W mice are a major site for the homeostasis of plasma cells. Eur J Immunol. 2001; 31:2726–2732. [PubMed: 11536171]
15. Mohr E, Serre K, Manz RA, Cunningham AF, Khan M, Hardie DL, Bird R, et al. Dendritic cells and monocyte/macrophages that create the IL-6/APRIL-rich lymph node microenvironments where plasmablasts mature. J Immunol. 2009; 182:2113–2123. [PubMed: 19201864]
16. Tokoyoda K, Zehentmeier S, Chang HD, Radbruch A. Organization and maintenance of immunological memory by stroma niches. Eur J Immunol. 2009; 39:2095–2099. [PubMed: 19637201]

17. Tedder TF, Engel P. CD20: a regulator of cell-cycle progression of B lymphocytes. Immunol Today. 1994; 15:450–454. [PubMed: 7524522]
18. Howard M, Grimaldi JC, Bazan JF, Lund FE, Santos-Argumedo L, Parkhouse RM, Walseth TF, et al. Formation and hydrolysis of cyclic ADP-ribose catalyzed by lymphocyte antigen CD38. Science. 1993; 262:1056–1059. [PubMed: 8235624]
19. Harada H, Kawano MM, Huang N, Harada Y, Iwato K, Tanabe O, Tanaka H, et al. Phenotypic difference of normal plasma cells from mature myeloma cells. Blood. 1993; 81:2658–2663. [PubMed: 8490175]
20. Jackson N, Ling NR, Ball J, Bromidge E, Nathan PD, Franklin IM. An analysis of myeloma plasma cell phenotype using antibodies defined at the IIIrd International Workshop on Human Leucocyte Differentiation Antigens. Clin Exp Immunol. 1988; 72:351–356. [PubMed: 3048803]
21. Terstappen LW, Hollander Z, Meiners H, Loken MR. Quantitative comparison of myeloid antigens on five lineages of mature peripheral blood cells. J Leukoc Biol. 1990; 48:138–148. [PubMed: 2196321]
22. Gershwin ME, Ansari AA, Mackay IR, Nakanuma Y, Nishio A, Rowley MJ, Coppel RL. Primary biliary cirrhosis: an orchestrated immune response against epithelial cells. Immunol Rev. 2000; 174:210–225. [PubMed: 10807518]
23. Gershwin ME, Mackay IR. The causes of primary biliary cirrhosis: Convenient and inconvenient truths. Hepatology. 2008; 47:737–745. [PubMed: 18098322]
24. Kamihira T, Shimoda S, Harada K, Kawano A, Handa M, Baba E, Tsuneyama K, et al. Distinct costimulation dependent and independent autoreactive T-cell clones in primary biliary cirrhosis. Gastroenterology. 2003; 125:1379–1387. [PubMed: 14598254]
25. Kamihira T, Shimoda S, Nakamura M, Yokoyama T, Takii Y, Kawano A, Handa M, et al. Biliary epithelial cells regulate autoreactive T cells: implications for biliary-specific diseases. Hepatology. 2005; 41:151–159. [PubMed: 15619239]
26. Kita H, Matsumura S, He XS, Ansari AA, Lian ZX, Van de Water J, Coppel RL, et al. Quantitative and functional analysis of PDC-E2-specific autoreactive cytotoxic T lymphocytes in primary biliary cirrhosis. J Clin Invest. 2002; 109:1231–1240. [PubMed: 11994412]
27. Krams SM, Dorshkind K, Gershwin ME. Generation of biliary lesions after transfer of human lymphocytes into severe combined immunodeficient (SCID) mice. J Exp Med. 1989; 170:1919–1930. [PubMed: 2584930]
28. Shigematsu H, Shimoda S, Nakamura M, Matsushita S, Nishimura Y, Sakamoto N, Ichiki Y, et al. Fine specificity of T cells reactive to human PDC-E2 163-176 peptide, the immunodominant autoantigen in primary biliary cirrhosis: implications for molecular mimicry and cross-recognition among mitochondrial autoantigens. Hepatology. 2000; 32:901–909. [PubMed: 11050037]
29. Shimoda S, Ishikawa F, Kamihira T, Komori A, Niiro H, Baba E, Harada K, et al. Autoreactive T-cell responses in primary biliary cirrhosis are proinflammatory whereas those of controls are regulatory. Gastroenterology. 2006; 131:606–618. [PubMed: 16890612]
30. Shimoda S, Nakamura M, Ishibashi H, Kawano A, Kamihira T, Sakamoto N, Matsushita S, et al. Molecular mimicry of mitochondrial and nuclear autoantigens in primary biliary cirrhosis. Gastroenterology. 2003; 124:1915–1925. [PubMed: 12806624]
31. Zhang W, Sharma R, Ju ST, He XS, Tao Y, Tsuneyama K, Tian Z, et al. Deficiency in regulatory T cells results in development of antimitochondrial antibodies and autoimmune cholangitis. Hepatology. 2009; 49:545–552. [PubMed: 19065675]
32. Lleo A, Selmi C, Invernizzi P, Podda M, Coppel RL, Mackay IR, Gores GJ, et al. Apotopes and the biliary specificity of primary biliary cirrhosis. Hepatology. 2009; 49:871–879. [PubMed: 19185000]
33. Fukushima N, Nalbandian G, Van De Water J, White K, Ansari AA, Leung P, Kenny T, et al. Characterization of recombinant monoclonal IgA anti-PDC-E2 autoantibodies derived from patients with PBC. Hepatology. 2002; 36:1383–1392. [PubMed: 12447863]
34. Malmborg AC, Shultz DB, Luton F, Mostov KE, Richly E, Leung PS, Benson GD, et al. Penetration and co-localization in MDCK cell mitochondria of IgA derived from patients with primary biliary cirrhosis. J Autoimmun. 1998; 11:573–580. [PubMed: 9802945]

35. Borchers AT, Shimoda S, Bowlus C, Keen CL, Gershwin ME. Lymphocyte recruitment and homing to the liver in primary biliary cirrhosis and primary sclerosing cholangitis. Semin Immunopathol. 2009; 31:309–322. [PubMed: 19533132]
36. Weninger W, Carlsen HS, Goodarzi M, Moazed F, Crowley MA, Baekkevold ES, Cavanagh LL, et al. Naive T cell recruitment to nonlymphoid tissues: a role for endothelium-expressed CC chemokine ligand 21 in autoimmune disease and lymphoid neogenesis. J Immunol. 2003; 170:4638–4648. [PubMed: 12707342]
37. Grant AJ, Lalor PF, Hubscher SG, Briskin M, Adams DH. MAdCAM-1 expressed in chronic inflammatory liver disease supports mucosal lymphocyte adhesion to hepatic endothelium (MAdCAM-1 in chronic inflammatory liver disease). Hepatology. 2001; 33:1065–1072. [PubMed: 11343233]
38. Grant AJ, Goddard S, Ahmed-Choudhury J, Reynolds G, Jackson DG, Briskin M, Wu L, et al. Hepatic expression of secondary lymphoid chemokine (CCL21) promotes the development of portal-associated lymphoid tissue in chronic inflammatory liver disease. Am J Pathol. 2002; 160:1445–1455. [PubMed: 11943728]
39. Isse K, Harada K, Zen Y, Kamihira T, Shimoda S, Harada M, Nakanuma Y. Fractalkine and CX3CR1 are involved in the recruitment of intraepithelial lymphocytes of intrahepatic bile ducts. Hepatology. 2005; 41:506–516. [PubMed: 15726664]
40. Shimoda S, Harada K, Niiro H, Taketomi A, Maehara Y, Tsuneyama K, Kikuchi K, et al. CX3CL1 (fractalkine): a signpost for biliary inflammation in primary biliary cirrhosis. Hepatology. 2010; 51:567–575. [PubMed: 19908209]
41. Goddard S, Williams A, Morland C, Qin S, Gladue R, Hubscher SG, Adams DH. Differential expression of chemokines and chemokine receptors shapes the inflammatory response in rejecting human liver transplants. Transplantation. 2001; 72:1957–1967. [PubMed: 11773896]
42. Shackel NA, McGuinness PH, Abbott CA, Gorrell MD, McCaughan GW. Identification of novel molecules and pathogenic pathways in primary biliary cirrhosis: cDNA array analysis of intrahepatic differential gene expression. Gut. 2001; 49:565–576. [PubMed: 11559656]
43. Terada R, Yamamoto K, Hakoda T, Shimada N, Okano N, Baba N, Ninomiya Y, et al. Stromal cell-derived factor-1 from biliary epithelial cells recruits CXCR4-positive cells: implications for inflammatory liver diseases. Lab Invest. 2003; 83:665–672. [PubMed: 12746476]
44. Buckley CD, Amft N, Bradfield PF, Pilling D, Ross E, Arenzana-Seisdedos F, Amara A, et al. Persistent induction of the chemokine receptor CXCR4 by TGF-beta 1 on synovial T cells contributes to their accumulation within the rheumatoid synovium. J Immunol. 2000; 165:3423–3429. [PubMed: 10975862]
45. Wright N, Hidalgo A, Rodriguez-Frade JM, Soriano SF, Mellado M, Parmo-Cabanas M, Briskin MJ, et al. The chemokine stromal cell-derived factor-1 alpha modulates alpha 4 beta 7 integrin-mediated lymphocyte adhesion to mucosal addressin cell adhesion molecule-1 and fibronectin. J Immunol. 2002; 168:5268–5277. [PubMed: 11994484]
46. Yasoshima M, Tsuneyama K, Harada K, Sasaki M, Gershwin ME, Nakanuma Y. Immunohistochemical analysis of cell-matrix adhesion molecules and their ligands in the portal tracts of primary biliary cirrhosis. J Pathol. 2000; 190:93–99. [PubMed: 10640998]
47. Takahashi T, Isemura M, Nakamura T, Matsui S, Oyanagi Y, Asakura H. Immunolocalization of a fibronectin-binding proteoglycan (PG-P1) immunologically related to HSPG2/perlecan in normal and fibrotic human liver. J Hepatol. 1994; 21:500–508. [PubMed: 7814795]
48. Matsui S, Takahashi T, Oyanagi Y, Takahashi S, Boku S, Takahashi K, Furukawa K, et al. Expression, localization and alternative splicing pattern of fibronectin messenger RNA in fibrotic human liver and hepatocellular carcinoma. J Hepatol. 1997; 27:843–853. [PubMed: 9382972]
49. Holt RU, Fagerli UM, Baykov V, Ro TB, Hov H, Waage A, Sundan A, et al. Hepatocyte growth factor promotes migration of human myeloma cells. Haematologica. 2008; 93:619–622. [PubMed: 18326526]
50. Yokomori H, Oda M, Ogi M, Wakabayashi G, Kawachi S, Yoshimura K, Nagai T, et al. Expression of adhesion molecules on mature cholangiocytes in canal of Hering and bile ductules in wedge biopsy samples of primary biliary cirrhosis. World J Gastroenterol. 2005; 11:4382–4389. [PubMed: 16038038]

51. Yokomori H, Oda M, Yoshimura K, Nomura M, Ogi M, Wakabayashi G, Kitajima M, et al. Expression of intercellular adhesion molecule-1 and lymphocyte function-associated antigen-1 protein and messenger RNA in primary biliary cirrhosis. Intern Med. 2003; 42:947–954. [PubMed: 14606706]

52. Oo YH, Adams DH. The role of chemokines in the recruitment of lymphocytes to the liver. J Autoimmun. 2010; 34:45–54. [PubMed: 19744827]

53. Kikuchi K, Hsu W, Hosoya N, Moritoki Y, Kajiyama Y, Kawai T, Takai A, et al. Ursodeoxycholic acid reduces CpG-induced IgM production in patients with primary biliary cirrhosis. Hepatol Res. 2009; 39:448–454. [PubMed: 19207576]

54. Hiepe F, Dorner T, Hauser AE, Hoyer BF, Mei H, Radbruch A. Long-lived autoreactive plasma cells drive persistent autoimmune inflammation. Nat Rev Rheumatol. 2011; 7:170–178. [PubMed: 21283146]

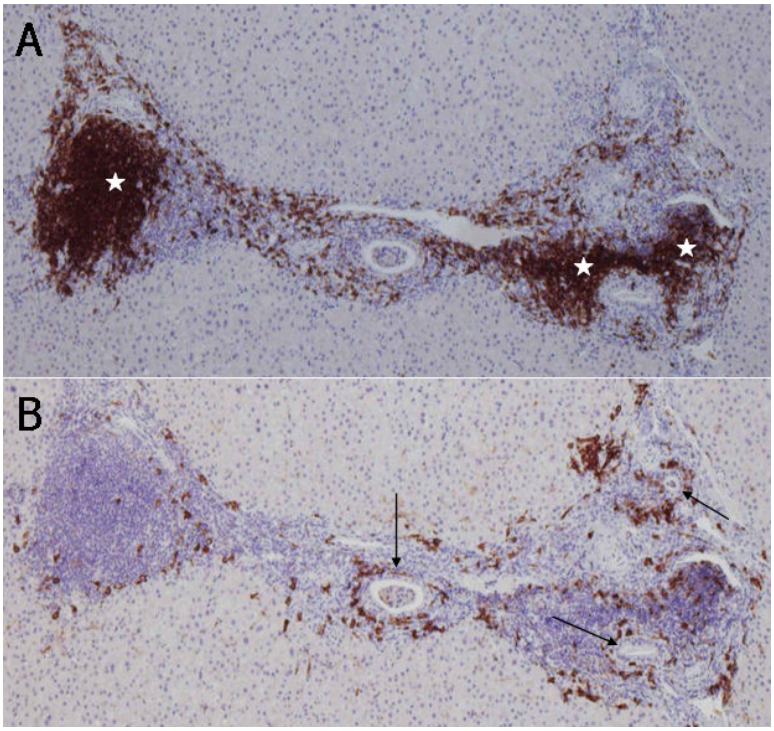

Figure 1.
Immunohistochemical staining of $CD20^+$ B lymphocytes and $CD38^+$ cells in consecutive sections of a PBC liver. A. $CD20^+$ B lymphocytes are either aggregated in lymph follicle-like structures (white stars) or scattered around inflamed portal tracts. B. Coronal arrangement (CA) of $CD38^+$ cells surrounding the intralobular bile ducts (arrows). Note that $CD38^+$ cells are scarce in lymph follicle-like structures. ABC method, x10.

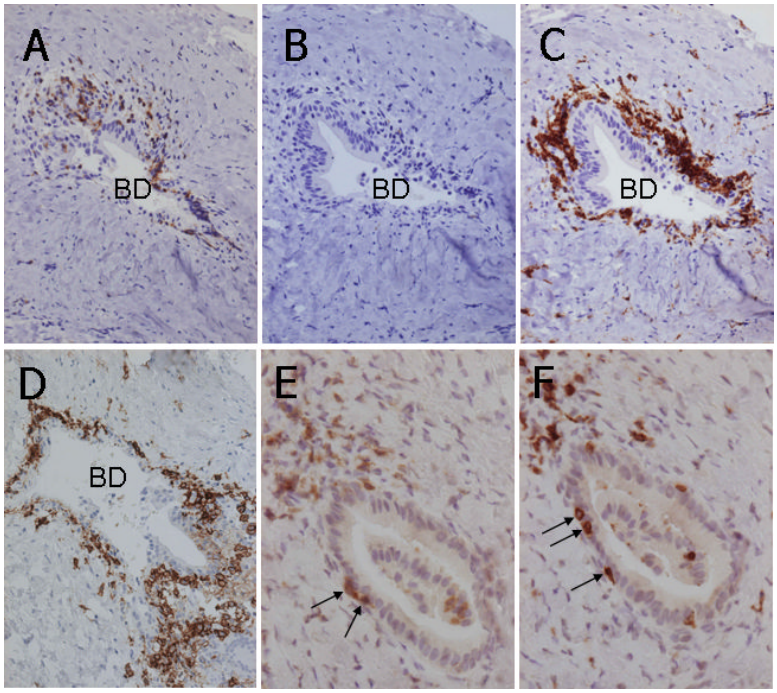

Figure 2.

Immunohistochemical staining of $CD3^+$ pan-T lymphocytes, $CD20^+$ B lymphocytes, $CD38^+$ cells, $CD4^+$ T lymphocytes and $CD8^+$ T lymphocytes in two sets of consecutive PBC liver sections. In the first consecutive section set (panels A, B, C and D), $CD3^+$ pan-T lymphocytes are scattered around an intrahepatic bile duct (BD) with CNSDC **(A)**; $CD20^+$ B lymphocytes are not observed around this intrahepatic bile duct (BD) **(B)**; while $CD38^+$ cells show distinct coronal arrangement surrounding this intrahepatic bile duct (BD) with CNSDC **(C)**. The coronal arrangement of $CD38^+$ cells is continuously observed along with CNSDC in serial sections. In subsequent serial consecutive sections (panels E and F), $CD4^+$ T lymphocytes (E) and $CD8^+$ T lymphocytes (F) demonstrate the same pattern of infiltration (arrows) into the cholangioepithelium of an intrahepatic bile duct (BD) with CNSDC. ABC method, x25.

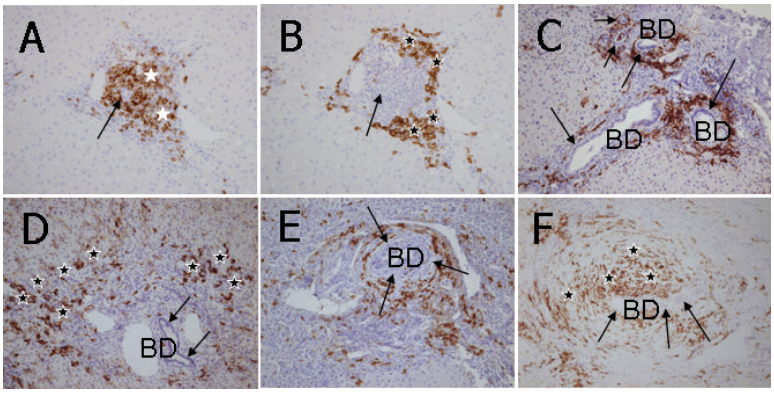

Figure 3.

Immunohistochemical staining of $CD20^+$ and $CD38^+$ cells in liver sections. **A.** In CH-C, $CD20^+$ B lymphocytes are aggregated in a follicle-like structure in an inflamed portal tract (white stars). Note that an intrahepatic bile duct (an arrow) is centered in such a follicle-like structure. **B.** In a consecutive section of CH-C liver (with panel A), $CD38^+$ cells are primarily located in the periphery of inflamed portal tracts (black stars) apart from the intrahepatic bile ducts (an arrow). **C.** In AIH, $CD38^+$ cells are not observed in the proximity of intrahepatic bile ducts (BD, arrows) but abundantly infiltrated in the area of interface hepatitis (black stars). **D.** In PBC, $CD38^+$ cells show the coronal arrangement surrounding intrahepatic bile ducts (BD) with CNSDC (arrows). **E.** In a case of stage 4 PSC, $CD38^+$ cells are surrounding the onion skin-like fibrosis that is a characteristic of PSC (arrows). This pattern is coined a satellite-like arrangement (SA) of $CD38^+$ cells surrounding concentric periductal fibrosis. The SA pattern is different from the CA of $CD38^+$ cells in PBC located just beneath the cholangioepithelium with CNSDC, as shown in Figures 2C and 4D. **F.** In a case of stage 1 PSC, $CD38^+$ cells are concentrically scattered in the onion skin-like fibrosis (black stars) surrounding an intrahepatic bile duct (arrows). This pattern is also regarded as SA of $CD38^+$ cells. ABC method, x25.

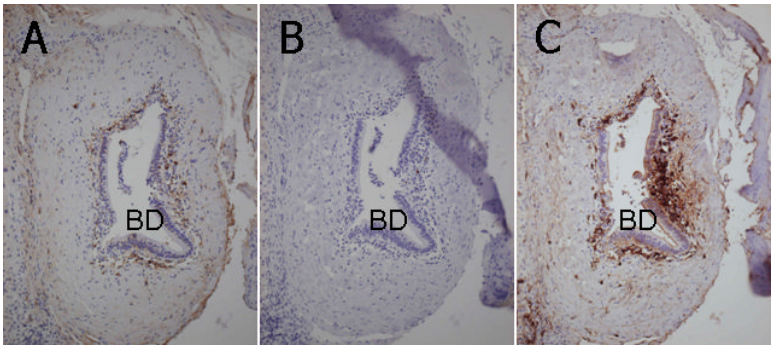

Figure 4.

Immunohistochemical staining of IgG, IgA and IgM in consecutive liver sections of a PBC liver. **A.** IgG^+ cells demonstrate a relatively loose coronal arrangement surrounding an intrahepatic bile duct (BD) with CNSDC. **B.** IgA^+ cells are not found in the vicinity of this intrahepatic bile duct (BD) with CNSDC. **C.** IgM^+ cells demonstrate a dense and distinct coronal arrangement surrounding this intrahepatic bile duct (BD) with CNSDC. Labeled streptavidin-biotin method, x25.

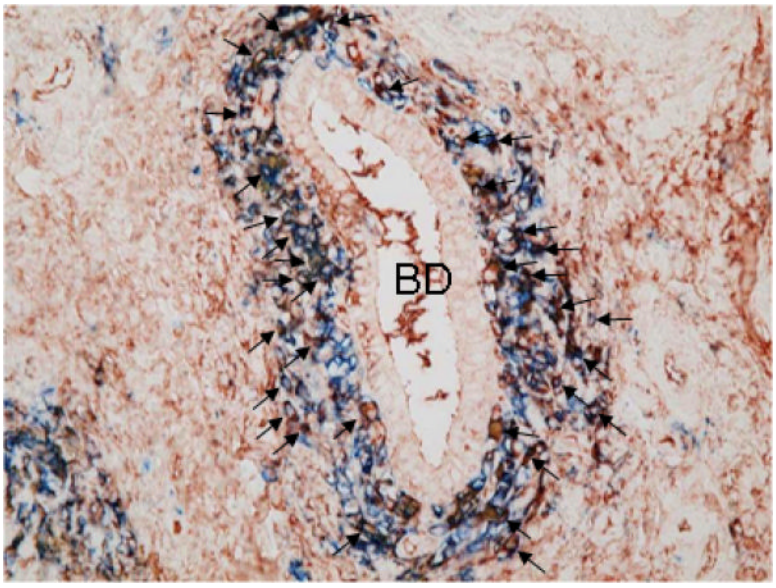

Figure 5.
Double immunostaining of CD38 and IgM in a PBC liver. The majority (approximately 70%) of $CD38^{+}$ cells that are immunohistochemically identified by a blue color (Fast blue) demonstrate a reddish brown color (AEC) in their cytoplasm indicating presence of intracellular IgM (arrows). BD: an intrahepatic bile duct with CNSDC, indirect double enzyme-antibody method, x100.

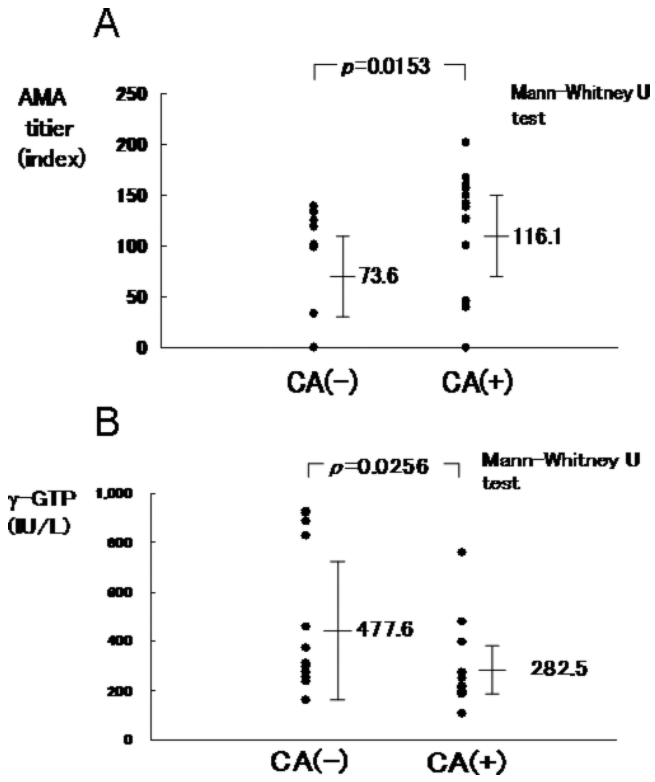

Figure 6.

AMA titers and γ-GTP levels in coronal arrangement (CA)-positive and CA-negative PBC patients . **A**. The titer of AMA is significantly higher in the CA-positive PBC patients compared to the CA-negative patients. **B**. γ-GTP level is significantly lower in the CA-positive PBC patients compared to CA-negative patients.

Table 1

Clinicopathological profiles of PBC, CH-C, AIH, PSC and GVHD subjects

	PBC n=26	CH-C n=27	AIH n=8	PSC n=8	GVHD n=9
Age (year)	57.2 ± 9.3	57.9 ± 11.3	59.5 ± 9.5	46.0 ± 24.6	45.9 ± 14.2[a]
Male/female	7/19	7/20	1/7	7/1	7/2
Scheuer stage (1/2/3/4)	15/3/8/0	--	--	--	--
Fibrosis score (0/1/2/3/4)	--	0/15/6/6/0	0/2/5/1/0	--	1/7/0/1/0
Activity score (0/1/2/3)	--	0/13/12/2	0/1/1/6	--	0/8/0/1
Ludwig stage (1/2/3/4)	--	--	--	5/1/1/1	--
Biopsy procedures (Echo/Laparo/Ope)	1/24/1	27/0/0	1/7/0	6/2/0	9/0/0
Evaluated portal tracts	12.2 ± 4.7[b]	15.2 ± 5.6[c]	13.0 ± 4.2[d]	9.0 ± 6.5	7.0 ± 2.5
Evaluated bile ducts	22.5 ± 11.4[e]	25.6 ± 11.6[f]	30.6 ± 19.8[g]	17.5 ± 15.1	12.0 ± 4.1
AST (IU/L)	99.3 ± 141.1	55.7 ± 40.9	332.1 ± 522.2[h]	111.9 ± 90.7	124.4 ± 140.8
ALT (IU/L)	105.2 ± 159.4	58.7 ± 42.4	333.4 ± 367.2[i]	126.4 ± 99.1[j]	217.4 ± 289.0[k]
ALP (IU/L)	775.7 ± 389.4[l]	251.2 ± 92.3	412.0 ± 156.9[m]	560.8 ± 627.2	434.2 ± 348.4
γ-GTP (IU/L)	380.1 ± 258.8[n]	48.7 ± 43.4	155.1 ± 36.4[o]	374.3 ± 269.8[p]	572.3 ± 668.7[q]

Numerical characters are expressed as mean ± standard deviation. Statistical significance with Mann-Whitney U test:

[a] p=0.0326 compared to that in PBC and p=0.0269 compared to that in CH-C and p=0.0377 compared to that in AIH

[b] p=0.0033 compared to that in GVHD

[c] p=0.0343 compared to that in PBC and p=0.0139 compared to that in PSC and p=0.0003 compared to that in GVHD

[d] p=0.0119 compared to that in GVHD

[e] p=0.0038 compared to that in GVHD

[f] p=0.0019 compared to that in GVHD

[g] p=0.0233 compared to that in GVHD

[h] p=0.0035 compared to that in PBC and p=0.0004 compared to that in CH-C

[i] p=0.0015 compared to that in PBC and p=0.0001 compared to that in CH-C and p=0.0460 compared to that in PSC

[j] $p=0.0148$ compared to that in CH-C

[k] $p=0.0184$ compared to that in CH-C

[l] $p<0.0001$ compared to that in CH-C and $p=0.0133$ compared to that in AIH and $p=0.0082$ compared to that in GVHD

[m] $p=0.0085$ compared to that in CH-C

[n] $p<0.0001$ compared to that in CH-C and $p=0.0008$ compared to that in AIH

[o] $p=0.0002$ compare to that in CH-C

[p] $p=0.0004$ compared to that in CH-C

[q] $p<0.0001$ compared to that in CH-C and $p=0.0433$ compared to that in AIH.

Table 2

Histological and immunohistological characteristics of the PBC, CH-C, AIH, PSC and GVHD livers

	PBC n=26		CH-C n=27		AIH n=8		PSC n=8		GVHD n=9	
	No. of cases	**%**	**No. of cases**	**%**	**No. of cases**	**%**	**No. of cases**	**%**	**No. of cases**	**%**
CNSDC	13	(50.0)	0	0	0	0	0	0	0	0
Granuloma	6	(23.1)	0	0	0	0	0	0	0	0
Lymph follicle-like infiltration*	6	(23.1)	12	(44.4)	2	(25.0)	0	0	0	0
Infiltration of $CD4^+$ cells into cholangioepithelium*	16	(61.5)	0	0	1	(12.5)	2	(25.0)	0	0
Infiltration of $CD8^+$ cells into cholangioepithelium*	7	(26.9)	4	(14.8)	3	(37.5)	1	(12.5)	7	(77.8*)
Coronal arrangement of $CD38^+$ cells	13	(50.0)	0	0	0	0	0	0	1	(11.1)
Coronal arrangement of IgG^+ cells	5	(19.2)	--	--	--	--	--	--	--	--
Coronal arrangement of IgM^+ cells	8	(30.8)	--	--	--	--	--	--	--	--
Coronal arrangement of IgG^+ and IgM^+ cells	3	(11.5)	--	--	--	--	--	--	--	--

*Statistical significance with Chi-square tests: p=0.0221 compared to PBC and p=0.0017 compared to that in CH-C and p=0.0275 compared to that in PSC.

Table 3

Coronal arrangement (CA) of $CD38^+$ cells and clinical data in PBC

	CA (-) n=13	CA (+) n=13	p
AST	88.6 ± 91.4	110.0 ± 181.3	0.8174
ALT	88.6 ± 79.1	121.8 ± 215.5	0.7778
ALP	789.8 ± 422.4	761.7 ± 370.3	1.0000
γ-GTP	477.6 ± 296.4	282.5 ± 176.2	0.0256*
TB	0.63 ± 0.22	0.71 ± 0.18	0.2012
TP	7.67 ± 0.5	8.02 ± 0.77	0.1635
Albumin	4.22 ± 0.31	4.35 ± 0.31	0.2668
TC	223.6 ± 34.7	195.1 ± 32.4	0.1059
TG	116.2 ± 56.8	111.5 ± 50.1	0.9795
IgG	1,728.3 ± 367.2	1,838.2 ± 529.4	0.7779
IgA	266.4 ± 79.4	298.5 ± 112.3	0.3428
IgM	293.5 ± 199.9	517.2 ± 438.3	0.0858
AMA titer	67.9 ± 61.8	119.5 ± 58.2	0.0153*
ANA titer	433.8 ± 791.3	163.1 ± 355	0.7163

CA (-): Without coronal arrangement of $CD38^+$ cells, CA (+): with coronal arrangement of $CD38^+$ cells.

*Mann-Whitney U test is applied and $p<0.05$ is significant.